




All-optical correlated noisy channel and its application in recovering quantum coherenceDan Lei, Disheng Guo , Jun Xin ,* and Xiao-Ming Lu †*Department of Physics, Hangzhou Dianzi University, Hangzhou 310018, China*

(Received 22 December 2023; accepted 24 May 2024; published 10 June 2024)

Attenuation and amplification are the most common processes for optical communications. Amplification can be used to compensate the attenuation of the complex amplitude of an optical field, but is unable to recover the coherence lost, provided that the attenuation channel and the amplification channel are independent. In this paper, we show that the quantum coherence of an optical field can be regained if the attenuation channel and the amplification channel share correlated noise. We propose an all-optical correlated noisy channel relying on the four-wave mixing process and demonstrate its capability of recovering quantum coherence within continuous-variable systems. We quantitatively investigate the coherence recovery phenomena for coherent states and two-mode squeezed states. Moreover, we analyze the effect of other photon losses that are independent from the recovery channel on the performance of recovering coherence. Different from correlated noisy channels previously proposed based on electro-optic conversions, the correlated noisy channel in our protocol is all-optical and thus owns larger operational bandwidths.

DOI: [10.1103/PhysRevA.109.062410](https://doi.org/10.1103/PhysRevA.109.062410)**I. INTRODUCTION**

Quantum coherence is a basic feature that marks the departure of the quantum realm from the classical world [1–3]. Arising from the superposition principle, quantum coherence embodies the essence of quantum correlations including quantum entanglement [4–6] and quantum steering [7]. As a resource for information processing [1–3], quantum coherence is fragile as decoherence inevitably occurs due to the interaction between a quantum system and its environment. Much effort has been devoted to mitigating the decoherence in discrete variable quantum systems, with notable examples including dynamical decoupling [8–10], error correcting codes [11–16], reservoir engineering [17], inversion of quantum jumps [18], and feedback control [19,20]. In addition to the discrete variable regime, continuous variable systems, such as quantum oscillators and optical fields, are also of great significance in quantum information processing [21].

Quantum correlation can be used against the noise effect during quantum information processing. When the noise channel has memory effect or shares correlation [22,23], it is possible to recover some quantum resources that are damaged due to decoherence. For example, revival of squeezing [24] and Einstein-Podolsky-Rosen (EPR) steering [25] have been observed in the experiment using correlated noisy channels. Such correlated noisy channels can also be used to implement some information processing tasks that are impossible by only using independent channels, e.g., Gaussian error correction can be fulfilled via correlated noisy channels [26].

Currently, correlated noisy channels are all established based on the conventional feed-forward techniques. It

employs the same signal generators to produce the correlated noise between the quantum system and environment, and then uses electro-optic modulators to perform the encoding and decoding procedures in classical channels [24–26]. However, such conventional correlated noisy channels are limited by the electrical bandwidth of the modulators. Note that the operational bandwidth is an important factor for the correlated noisy channel. This is because the quantum properties (e.g., quantum coherence) of a quantum system may be distributed within a large range of the frequency spectrum. To recover the quantum properties of a quantum system that passes through a noisy channel, the operational bandwidth of the correlated noisy channel should match with that of the noisy channel. Therefore, it is valuable to further enhance the operational bandwidth of the correlated noisy channel. This leads us to explore an all-optical version of the correlated noisy channel.

In this paper, we propose an all-optical correlated noisy channel (ACNC) based on four-wave mixing (FWM) processes in hot atomic ensembles and to investigate its capability of recovering quantum coherence. Different from conventional correlated noisy channels, the ACNC avoids the electro-optic conversions and its noisy channels are all-optical. Due to the unique advantage of the all-optical strategy [27,28], the ACNC owns larger operational bandwidth than the conventional correlated noisy channels. We use the ACNC to recover the coherence loss of an optical field, that is caused by the attenuation modeled by beam splitting. A common amplification process can compensate the attenuation of the complex amplitude of an optical field but cannot recover the loss of coherence. The amplification even brings in excessive noise [29–32]. We shall show that, utilizing the correlated noise in the attenuation channel and the amplification channel, the ACNC can recover a portion of coherence while compensating the loss of the complex amplitude. We use the Gaussian relative entropy of coherence [33] as a coherence measure to

*jxin@hdu.edu.cn

†lxm@hdu.edu.cn

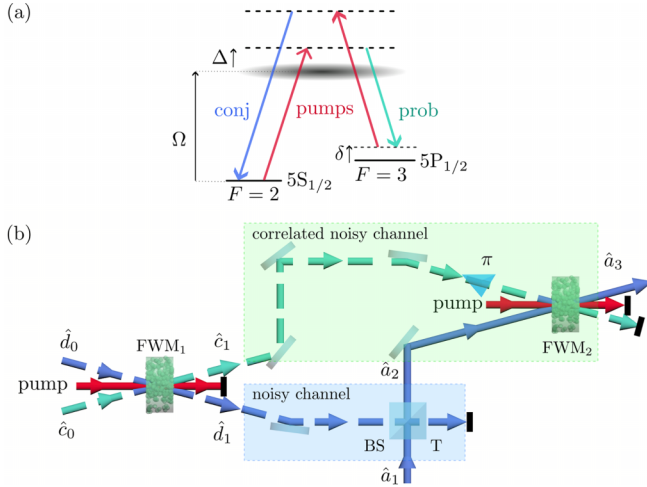


FIG. 1. (a) Energy-level diagram for the FWM process: conj, conjugate; prob, probe; Δ , one-photon detunings; δ , two-photon detuning; Ω , resonant Rabi frequency. The width of the excited state represents the Doppler-broadened profile. (b) Design of the ACNC based on BS and FWM.

quantitatively study the coherence recovery for coherent states and two-mode squeezed states (TMSSs). In addition, we also investigate the effect of imperfect factors on the performance of the ACNC, such as the photon absorption occurring in the atomic cells and unavoidable losses in the light path.

This paper is organized as follows. In Sec. II, we give the design of the ACNC and all the relevant input-output relations for the processes therein. In Sec. III, we give a brief review on the coherence measure for Gaussian states and then study the capability of the ACNC for recovering the quantum coherence of a single-mode coherent state and a TMSS. We also analyze the impact of photon loss. We summarize our paper in Sec. IV.

II. ACNC BASED ON FWM PROCESSES

Figure 1 illustrates the configuration of ACNC, which employs two FWM processes and a beam splitting process. The first one (FWM₁) generates the correlated noise, while the second one (FWM₂) serves as a decoder that uses the quantum correlation produced from FWM₁ to recover the coherence of the quantum system. Under the “undepleted pump” approximation [34], the interaction Hamiltonian of FWM₁ is of the form $\hat{H}_1 = i\hbar\xi_1(\hat{c}_1\hat{d}_1 - \hat{c}_1^\dagger\hat{d}_1^\dagger)$, where the parameter ξ_1 is the interaction strength of FWM₁, and \hat{c}_1 and \hat{d}_1 are the annihilation operators of the probe and conjugate modes, respectively. This interaction Hamiltonian guarantees that the photons in modes \hat{c}_1 and \hat{d}_1 are produced simultaneously, and therefore strong quantum correlations will be generated between these two modes. The input-output relationship of FWM₁ is

$$\hat{c}_1 = G_1\hat{c}_0 + g_1\hat{d}_0^\dagger, \quad (1)$$

$$\hat{d}_1 = G_1\hat{d}_0 + g_1\hat{c}_0^\dagger, \quad (2)$$

where \hat{c}_0 and \hat{d}_0 are the annihilation operators for the two input modes of FWM₁, respectively, $G_1 = \cosh(\xi_1\tau)$ is the amplitude gain of FWM₁ with τ being the interaction

timescale, and $g_1 \equiv \sqrt{G_1^2 - 1}$. When the input modes \hat{c}_0 and \hat{d}_0 are in vacuum (i.e., FWM₁ is driven by the pump beam only), the output state is known as the EPR entangled state [35,36]. It has been shown that both the position and momentum quadratures of either \hat{c}_1 or \hat{d}_1 yield thermal noise. However, we can use the EPR correlation to reduce such thermal noise via a joint homodyne measurement [37].

We now consider a single-mode Gaussian optical field, denoted as \hat{a}_1 , that passes through a noisy channel that is realized by mixing \hat{a}_1 with \hat{d}_1 on a linear beam splitter (BS) with the transmissivity T . The input-output relation of the BS is

$$\hat{a}_2 = \sqrt{T}\hat{a}_1 + \sqrt{1-T}\hat{d}_1, \quad (3)$$

$$\hat{d}_2 = \sqrt{1-T}\hat{a}_1 - \sqrt{T}\hat{d}_1, \quad (4)$$

where \hat{a}_2 is taken as the output of the noisy channel and the other output mode \hat{d}_2 of the BS will not be considered. After the BS, the noise owned by \hat{d}_1 is injected into the optical field \hat{a}_1 and thus may destroy the coherence of the input quantum state.

To recovery the Gaussian information of mode \hat{a}_1 , we then use \hat{a}_2 as the input mode of FWM₂ driven by another pump beam, while the other port of FWM₂ is seeded by the mode \hat{c}_1 with a phase delay ϕ . The input-output relation of FWM₂ is

$$\hat{a}_3 = G_2\hat{a}_2 + g_2e^{i\phi}\hat{c}_1^\dagger, \quad (5)$$

$$\hat{c}_2 = G_2e^{-i\phi}\hat{c}_1 + g_2\hat{a}_2^\dagger, \quad (6)$$

where G_2 is the amplitude gain of FWM₂ and $g_2 \equiv \sqrt{G_2^2 - 1}$. We take \hat{a}_3 as the final output mode. Substituting Eqs. (1)–(3) into Eq. (7), \hat{a}_3 can be expressed with respect to the initial modes as

$$\begin{aligned} \hat{a}_3 = & G_2\sqrt{T}\hat{a}_1 + (G_1G_2\sqrt{1-T} + g_1g_2e^{i\phi})\hat{d}_0 \\ & + (G_2g_1\sqrt{1-T} + G_1g_2e^{i\phi})\hat{c}_0^\dagger. \end{aligned} \quad (7)$$

To compensate the amplitude loss of \hat{a}_1 , we henceforth set $G_2 = 1/\sqrt{T}$ so that $\hat{a}_3 = \hat{a}_1$ for $\hat{c}_0 = \hat{d}_0 = 0$. Moreover, it can be seen from Eq. (7) that extra noise is introduced by modes \hat{d}_0 and \hat{c}_0 . To simply this extra noise, we take $\phi = \pi$ throughout this paper. As a result, Eq. (7) can be rewritten as

$$\hat{a}_3 = \hat{a}_1 + g_2(G_1 - g_1)(\hat{d}_0 - \hat{c}_0^\dagger). \quad (8)$$

Note that the last term in Eq. (8) vanishes in the limit of $G_1 \gg 1$, meaning that the additive noise introduced by modes \hat{c}_1 and \hat{d}_1 can be approximately canceled when the intensity gain of FWM₁ is large enough.

The above-mentioned noise cancellation can be qualitatively explained as follows. First, recall that the modes \hat{c}_1 and \hat{d}_1 share correlated noises. This quantum correlation is then transferred so that the modes \hat{a}_2 and \hat{c}_1 become correlated after the combination of \hat{a}_1 and \hat{d}_1 performed in the BS. Finally, interference-induced quantum noise cancellation occurs as the internal degree of the amplifier (i.e., FWM₂) is correlated with the input signal mode [38]. Therefore, an ACNC is established. We can use the ACNC to recover the quantum information of the state of the initial input mode \hat{a}_1 .

Discussions of experimental feasibility

In the experiment, the FWM process can be realized by seeding a high-intensity pump beam into a hot Rb-85 [35,39–41] or CS-133 [42–44] vapor cell. This causes the generation of correlated probe (prob) and conjugate (conj) photons, which propagate at small angles with respect to the pump beam as shown in Fig. 1(b). The phase-matching condition of the FWM process requires both energy conservation and momentum conservation as follows: $2\omega_{\text{pump}} - \omega_{\text{prob}} - \omega_{\text{conj}} = 0$ and $2\vec{k}_{\text{pump}} - \vec{k}_{\text{prob}} - \vec{k}_{\text{conj}} = 0$, where ω_i and \vec{k}_i denote the frequency and wave vector of the corresponding photon [45]. Take the FWM process based on Rb-85 as an example as shown in Fig. 1(a). The pump beams are blue detuned about 0.8 GHz (single-photon detuning Δ) from the Rb-85 D_1 line ($5S_{1/2}, F = 2 \rightarrow 5P_{1/2}$) transition at 795 nm, where the resonant Rabi frequency Ω is not resolved due to the Doppler broadening. The generated probe and conjugate beams are red detuned about 3 GHz and blue detuned about 3 GHz from the pump beam, due to the phase-matching condition. The efficiency of the FWM process is dependent on various experimental parameters, such as pump power, single-photon detuning, and temperature of the atomic cell. Take single-photon detuning Δ as an example. When $\Delta \rightarrow 0$, the FWM process may be enhanced but its efficiency may also be limited by the absorptive loss [46,47], due to the electromagnetically induced transparency [48,49]. More details of experimental realizations of the FWM process can be found in Refs. [50–53].

As shown in Fig. 1(b), it should be noted the input modes \hat{d}_0 and \hat{c}_0 are in vacuum and FWM₁ is driven by the pump beam only. In this way, there are many output modes of FWM₁ meeting the phase-matching condition, which will lead to the conical emission after FWM₁ [54–56]. Nevertheless, we argue that such conical emission can never affect our ACNC scheme, due to the interference-induced mode selection occurring on both BS and FWM₂ [57]. The operator \hat{c}_1 (\hat{d}_1) in Eqs. (1)–(4) denotes the mode that satisfies the mode matching condition with \hat{a}_1 (\hat{a}_2). The rest modes in the conical emission will be abandoned via the interference.

In addition, phase locking technique should be involved in the ACNC scheme, which controls the phase between the noisy channel (FWM₁) and the correlated noisy channel (FWM₂). In the real implementation, the two FWM processes can be pumped by the beams from the same sources. And phase difference between modes \hat{c}_1 and \hat{a}_2 is required to be π . Since the input modes of FWM₁ are in vacuum, its output modes \hat{c}_1 and \hat{d}_1 are of zero quadrature means. Thus, it will be difficult to control the phase between modes \hat{c}_1 and \hat{a}_2 . Nevertheless, such issue can be solved by the quantum noise locking (QNL) technique [58], which can lock the relative phase between a squeezed vacuum state with zero quadrature means and a coherent state. Besides, it is also interesting to consider the effect of Doppler broadening of the FWM processes on the phase locking. The Doppler broadening, which is caused by the thermal motion of the atoms inside the hot vapor cell, will introduce extra noise into the error signal and thus degrades the stability of the QNL. To reduce the Doppler broadening, one can reduce the angle between the probe and pump beams or adjust the two-photon detuning

δ in the experiment [45]. However, this would also degrade the efficiency of the FWM process. Therefore, there will be a tradeoff between the reduction of Doppler broadening and the efficiency of the FWM process in the experiment.

III. RECOVERING QUANTUM COHERENCE VIA ACNC

A. Coherence measure for Gaussian states

We use quantum coherence [1,2] as an evaluating indicator to quantitatively investigate the recovery capability of the ACNC for the continuous-variable quantum information. We shall give a brief review on the quantum coherence of Gaussian states. Baumgratz, Cramer, and Plenio defined the quantum coherence of a quantum state $\hat{\rho}$ as the minimum distance measured by the quantum relative entropy between the quantum state and an incoherent state in the Hilbert space [1]. Denote by \mathcal{I} the set of all incoherent states whose density matrices are diagonal in the fixed reference basis. The relative entropy of coherence is defined as [1]

$$C_r(\hat{\rho}) = \min_{\hat{\sigma} \in \mathcal{I}} S(\hat{\rho} || \hat{\sigma}), \quad (9)$$

where $S(\hat{\rho} || \hat{\sigma}) = \text{tr}(\hat{\rho} \log_2 \hat{\rho}) - \text{tr}(\hat{\rho} \log_2 \hat{\sigma})$ is the quantum relative entropy between $\hat{\rho}$ and $\hat{\sigma}$. The relative entropy of coherence can be expressed as

$$C_r(\hat{\rho}) = S(\hat{\rho}_{\text{diag}}) - S(\hat{\rho}), \quad (10)$$

where $S(\hat{\rho}) = -\text{tr}(\hat{\rho} \log_2 \hat{\rho})$ is the von Neumann entropy of $\hat{\rho}$ and $\hat{\rho}_{\text{diag}}$ denotes the diagonal matrix obtained by removing all off-diagonal elements from $\hat{\rho}$ in the reference basis [1]. The relative entropy of coherence also serves as a well-defined quantifier for quantum coherence in infinite-dimensional bosonic systems [59].

For Gaussian states of a bosonic system, Xu [33] gave an alternative coherence measure—the Gaussian relative entropy of coherence:

$$C(\hat{\rho}) = \min_{\hat{\sigma} \in \mathcal{I}'} S(\hat{\rho} || \hat{\sigma}), \quad (11)$$

where \mathcal{I}' denotes the set of all incoherent Gaussian states with respect to the multimode Fock basis. Moreover, Xu showed that the closest incoherent Gaussian state to a N -mode Gaussian state $\hat{\rho}$ is the N -mode thermal state:

$$\hat{\rho}_{\text{th}} = \bigotimes_{j=1}^N \left[\sum_{n=0}^{\infty} \frac{\bar{n}_j^n}{(\bar{n}_j + 1)^{n+1}} |n\rangle \langle n| \right], \quad (12)$$

where \bar{n}_j is the mean number of photons in the j th mode. Therefore, the Gaussian relative entropy of coherence can be expressed as

$$C(\hat{\rho}) = S(\hat{\rho}_{\text{th}}) - S(\hat{\rho}). \quad (13)$$

The von Neumann entropy of the N -mode thermal state can be directly calculated as

$$S(\hat{\rho}_{\text{th}}) = \sum_{j=1}^N [(\bar{n}_j + 1) \log_2(\bar{n}_j + 1) - \bar{n}_j \log_2 \bar{n}_j]. \quad (14)$$

The von Neumann entropy of N -mode Gaussian states can be expressed as

$$S(\hat{\rho}) = \sum_{j=1}^N \left(\frac{\nu_j + 1}{2} \log_2 \frac{\nu_j + 1}{2} - \frac{\nu_j - 1}{2} \log_2 \frac{\nu_j - 1}{2} \right), \quad (15)$$

where ν_j is the symplectic eigenvalue of the covariance matrix V [60,61]. The entries of V are defined by $V_{ij} = \frac{1}{2} \langle \hat{x}_i \hat{x}_j + \hat{x}_j \hat{x}_i \rangle - \langle \hat{x}_i \rangle \langle \hat{x}_j \rangle$, where $\langle \bullet \rangle$ denotes the quantum expectation and $\hat{x} = (\hat{X}_1, \hat{P}_1, \dots, \hat{X}_N, \hat{P}_N)^T$ with $\hat{X}_j = \hat{a}_j + \hat{a}_j^\dagger$ and $\hat{P}_j = i(\hat{a}_j^\dagger - \hat{a}_j)$. It can be computed as the absolute value of the eigenvalues of the matrix $i\Omega V$, where $\Omega = \bigoplus_{k=1}^N \begin{pmatrix} 0 & 1 \\ -1 & 0 \end{pmatrix}$ is the symplectic transformation matrix.

B. Recovering quantum coherence of a coherent state

We now consider the capability of the ACNC in recovering the quantum coherence when the input state of the \hat{a}_1 mode is a coherent state $|\alpha\rangle$ and the states of \hat{c}_0 and \hat{d}_0 are the vacuum states. Let us denote by $\hat{\rho}_{a_1}$, $\hat{\rho}_{a_2}$, and $\hat{\rho}_{a_3}$ the quantum states of the modes \hat{a}_1 , \hat{a}_2 , and \hat{a}_3 , respectively. These states are all Gaussian, so we can use Eqs. (13)–(15) with Eqs. (3) and (8) to calculate their Gaussian relative entropy of coherence. Since the input state $|\alpha\rangle$ is a pure state whose von Neumann entropy vanishes, the quantum coherence of the input state is just $S(\hat{\rho}_{\text{th}})$ given by Eq. (14) with $N = 1$ (viz., the single mode case) and $n_1 = |\alpha|^2$. After the noisy channel modeled by the BS, the mean photon number is

$$\hat{a}_2^\dagger \hat{a}_2 = T|\alpha|^2 + (1-T)g_1^2, \quad (16)$$

from which we can obtain $S(\hat{\rho}_{\text{th}})$ via Eq. (14). Meanwhile, the covariance matrix for (\hat{X}_2, \hat{P}_2) is given by

$$V_{11} = V_{22} = 1 + 2(1-T)g_1^2, \quad (17)$$

$$V_{12} = V_{21} = 0. \quad (18)$$

The symplectic eigenvalue of the covariance matrix is $\nu_1 = 1 + 2(1-T)g_1^2$, with which we can obtain the von Neumann entropy of $\hat{\rho}_{a_2}$. After the ACNC, the mean photon number in the \hat{a}_3 mode is

$$\hat{a}_3^\dagger \hat{a}_3 = |\alpha|^2 + g_2^2(G_1 - g_1)^2 \quad (19)$$

and the covariance matrix for (\hat{X}_3, \hat{P}_3) is given by

$$V_{11} = V_{22} = 1 + 2g_2^2(G_1 - g_1)^2, \quad (20)$$

$$V_{12} = V_{21} = 0. \quad (21)$$

As shown in Fig. 2, the quantum coherence of $\hat{\rho}_{a_2}$ is smaller than that of $\hat{\rho}_{a_1}$ and decreases with the increase of G_1 . It means that the noisy channel destroys the quantum coherence of \hat{a}_1 and the decoherence becomes more obvious with the increase of the thermal noise introduced. On the other hand, the quantum coherence of $\hat{\rho}_{a_2}$, which is the output state of the ACNC, can be partially recovered and approaches to the quantum coherence of $\hat{\rho}_{a_1}$ with increasing G_1 . In other words, the decoherence caused by the noisy channel can be mitigated by the ACNC. When $G_1 \rightarrow \infty$, the quantum coherence of \hat{a}_1 can be totally recovered.

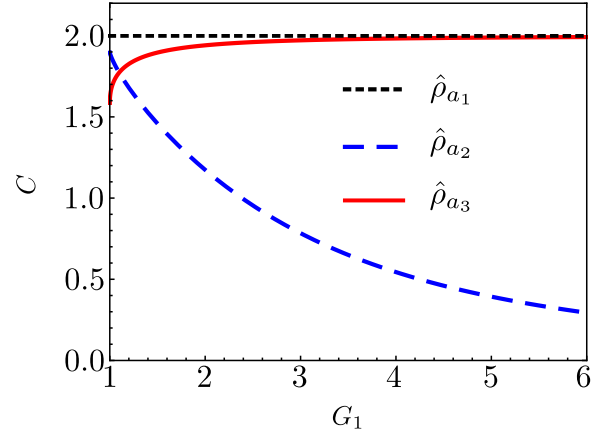


FIG. 2. Quantum coherence of a coherent state transmitted in quantum channels. Here, $\hat{\rho}_{a_1}$ is the initial state, ρ_{a_2} is the output state of the first noisy channel modeled by a beam splitter, and ρ_{a_3} is the output state of the ACNC. The parameters in plotting this figure are $\alpha = 1$, $G_2 = 1/\sqrt{T}$, and $T = 0.9$.

Effect of losses

In the above discussions, we have introduced two types of quantum channels, that is, the noisy channel and the ACNC. The noisy channel results in decoherence of the input Gaussian state, while the ACNC is capable of recovering the quantum coherence of the state that is degraded by the noisy channel. In the realistic scenario, the performance of the ACNC will be affected by unavoidable losses, such as atomic absorption during the FWM processes and losses in light paths [62,63]. In the following, we study how the losses affect the performance of the ACNC on coherence recovery. We model the lossy process as a BS with transmissivity η and use $L \equiv 1 - \eta$ to quantify the strength of loss. When an optical field \hat{a}_j passes through the lossy channel, it becomes $\hat{a}_j \rightarrow \sqrt{\eta_j} \hat{a}_j + \sqrt{1 - \eta_j} \hat{v}_j$, where \hat{v}_j is the annihilation operator for the other input port of the BS. The state of the mode \hat{v}_j is the vacuum state.

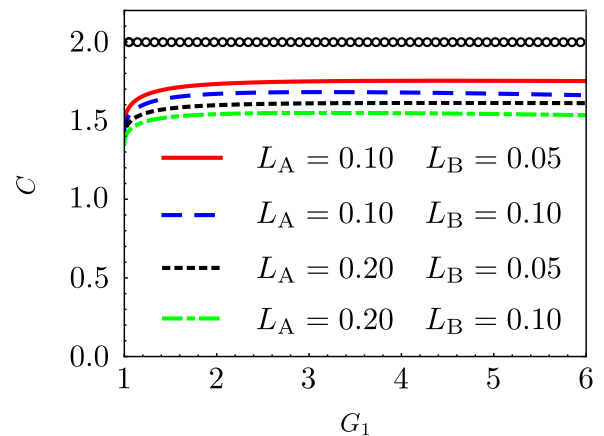


FIG. 3. Quantum coherence of the mode \hat{a}_3 vs G_1 under various losses. The circles denote the quantum coherence of the initial coherent state $\hat{\rho}_{a_1}$ for the convenience of comparison. The parameters in plotting this figure are $\alpha = 1$, $G_2 = 1/\sqrt{T}$, and $T = 0.9$.

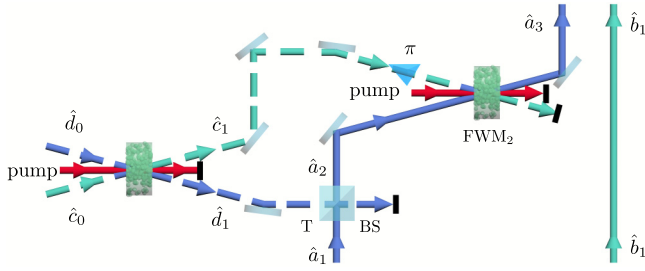


FIG. 4. Recovering quantum coherence of a TMSS via ACNC.

To describe the atomic absorption during the FWM processes, we assume that each of the modes \hat{a}_1 , \hat{c}_1 , and \hat{a}_3 , which are the relevant outputs of the involved FWMs, undergoes a lossy channel with the strength L_A . We also assume that there is a photon loss with the strength L_B occurring in the propagating mode \hat{a}_2 . We consider the situations where the loss caused by atomic absorption is of 10–20% and the loss in the light path is of 5–10%, as they give realistic experimental losses [63]. We plot in Fig. 3 the quantum coherence of the mode \hat{a}_3 versus G_1 for different loss strengths. Our results show that the ACNC cannot totally recover the quantum coherence of the mode \hat{a}_3 from that of the input mode \hat{a}_1 (which is of value 2) in the presence of losses. This is because the extra noise added by photon loss is uncorrelated. Different from the correlated noisy channel, the quantum decoherence caused by photon loss cannot be mitigated in principle.

C. Recovering quantum coherence of a TMSS

In the above, we have shown that the ACNC is able to recover the quantum coherence of coherent states undergoing a noisy channel. We now generalize our model to bipartite quantum systems. For a two-mode quantum state $\hat{\rho}_{AB}$, its total quantum coherence $C_t(\hat{\rho}_{AB}) \equiv C(\hat{\rho}_{AB})$ can be decomposed into two parts: the local coherence and the correlated coherence [64]. The local coherence of $\hat{\rho}_{AB}$ is defined as

$$C_l(\hat{\rho}_{AB}) \equiv C(\hat{\rho}_A) + C(\hat{\rho}_B), \quad (22)$$

where $C(\hat{\rho}_A)$ and $C(\hat{\rho}_B)$ are quantum coherence of the reduced density operators of the modes A and B , respectively.

In general, it is not necessary that all quantum coherence of a bipartite quantum system is stored locally. A part of quantum coherence may be stored in the correlation between the subsystems. The difference between total coherence $C_t(\hat{\rho}_{AB})$ and local coherence $C_l(\hat{\rho}_{AB})$ is defined as correlated coherence [64], which is denoted by $C_c(\hat{\rho}_{AB})$, i.e.,

$$C_c(\hat{\rho}_{AB}) \equiv C_t(\hat{\rho}_{AB}) - C_l(\hat{\rho}_{AB}). \quad (23)$$

As shown in Fig. 4, we consider a TMSS denoted by $\hat{\rho}_{a_1 b_1}$ as the input state of the noisy channel. In experiment, the quantum state $\hat{\rho}_{a_1 b_1}$ can be generated by a two-beam phase sensitive FWM process [65] with the input-output relations

$$\hat{a}_1 = G_0 \hat{a}_0 + e^{i\theta} g_0 \hat{b}_0^\dagger, \quad \hat{b}_1 = G_0 \hat{b}_0 + e^{i\theta} g_0 \hat{a}_0^\dagger, \quad (24)$$

where \hat{a}_0 and \hat{b}_0 are the input modes of the FWM process and are both assumed to be in coherent states, the parameter θ denotes the phase of the two-beam phase sensitive FWM process, G_0 is the amplitude gain, and $g_0 \equiv \sqrt{G_0^2 - 1}$. It has been shown that interference-induced quantum squeezing can be achieved by such a TMSS. Moreover, the quantum squeezing reaches its maximum when $\theta = 0$, corresponding to the bright interference fringe of the output ports of the FWM process.

To study the performance of the ACNC in recovering the quantum coherence of a TMSS, we first seed mode \hat{a}_1 into the noisy channel whose output mode is denoted by \hat{a}_2 . After the noisy channel, we seed mode \hat{a}_2 into the ACNC. Similar with the single-mode case as shown in Fig. 1, the noisy channel is realized by mixing mode \hat{a}_1 with \hat{d}_1 and the associated ACNC is realized by FWM₂, which uses correlated modes \hat{a}_2 and \hat{c}_1 as its input. The output of \hat{a}_3 can be written as

$$\hat{a}_3 = G_0 \hat{a}_0 + e^{i\theta} g_0 \hat{b}_0^\dagger + g_2(G_1 - g_1)(\hat{d}_0 - \hat{c}_0^\dagger). \quad (25)$$

We plot in Fig. 5 the total quantum coherence, the local quantum coherence, and the correlated quantum coherence for the bipartite state at different stages. As shown in Fig. 5(a), the effects of the noisy channel and the ACNC on the total quantum coherence of the TMSS are similar with that of the single-mode coherent state, which is shown in Fig. 2. It demonstrates that the ACNC can recover not only the quantum coherence of a single-mode coherent state undergoing the noisy channel but also the total quantum coherence of

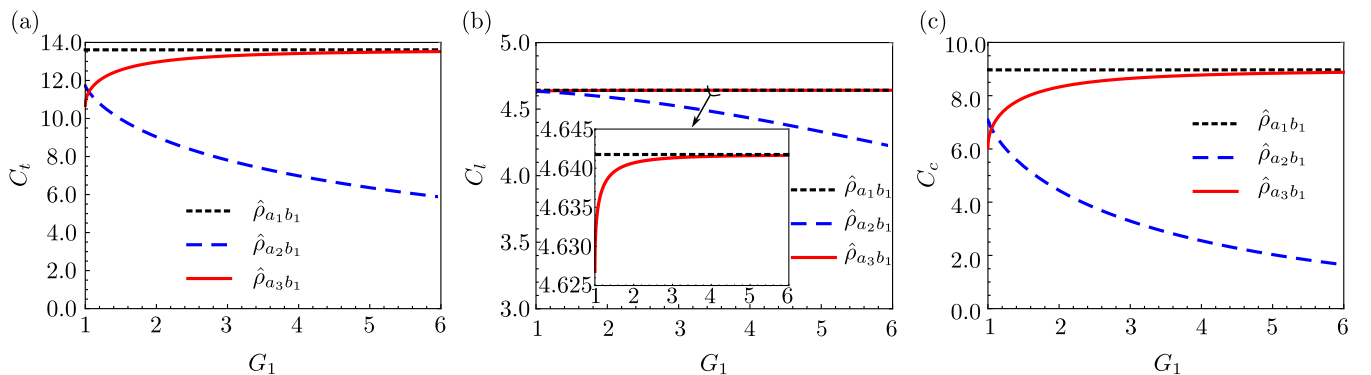


FIG. 5. Different kinds of quantum coherence of a TMSS transmitted via the noise channels and its ACNC. (a) Total quantum coherence. (b) Local quantum coherence. (c) Correlated quantum coherence. The black dotted line corresponds to the quantum coherence of the initial TMSS $\hat{\rho}_{a_1 b_1}$. The parameters in plotting this figure are $\theta = 0$, $G_0 = 3$, $G_2 = 1/\sqrt{T}$, and $T = 0.9$. The initial state of the FWM that generates the TMSS is $|\alpha\rangle \otimes |\alpha\rangle$ with $\alpha = 1$.

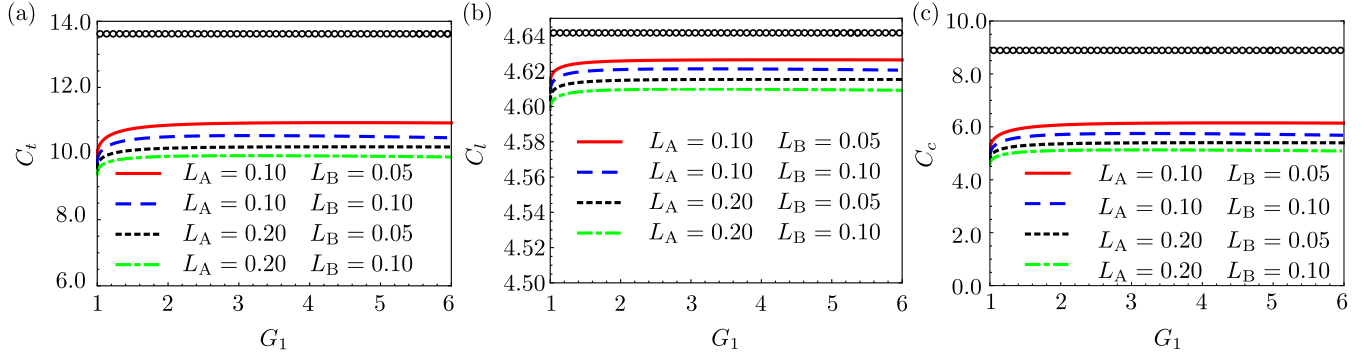


FIG. 6. Effect of losses on the performance of the ACNC in recovering the quantum coherence of a TMSS. (a) Total quantum coherence. (b) Local quantum coherence. (c) Correlated quantum coherence. The circle indicates the quantum coherence of the initial TMSS $\hat{\rho}_{a_1b_1}$ for the convenience of comparison. The parameters in plotting this figure are $\theta = 0$, $G_0 = 3$, $G_2 = 1/\sqrt{T}$, and $T = 0.9$. The initial state of the FWM that generates the TMSS is $|\alpha\rangle \otimes |\alpha\rangle$ with $\alpha = 1$.

a bipartite system whose subsystem is undergoing the noisy channel. Comparing Figs. 5(b) and 5(c), it can be seen that the local coherence of the TMSS is more robust against the noisy channel than the correlated coherence. Moreover, the local coherence of the TMSS can be almost recovered by the ACNC as long as $G_1 > 1$; the correlated coherence of $\hat{\rho}_{a_3b_1}$, however, can approach to that of the input state $\hat{\rho}_{a_1b_1}$ only if G_1 is large enough.

Effect of losses

We show in Fig. 6 the effect of losses on the performance of the ACNC in recovering the quantum coherence of the TMSS. We first focus on the local coherence. As shown in Fig. 6(b), the local coherences for different lossy cases are almost the same and all of them are very close to that of the input state $\hat{\rho}_{a_1b_1}$. It means that the local coherence of the TMSS has good robustness against losses. Different from the local coherence, the correlated coherence is vulnerable to the losses. As shown in Fig. 6(c), the correlated coherence of the state $\hat{\rho}_{a_3b_1}$ decreases rapidly with the increase of the losses. The ACNC can never recover the quantum coherence of the state $\hat{\rho}_{a_3b_1}$ to that of the input state $\hat{\rho}_{a_1b_1}$ as long as losses are involved.

IV. CONCLUSION

In this paper, we have proposed an ACNC relying on FWM processes and showed that the ACNC can utilize the correlated noise to recover a portion of coherent loss while amplifying the complex amplitude to compensate the attenuation.

The protocol has good performance for not only single-mode coherent states but also the TMSS. By dividing the total coherence of the TMSS into the local coherence and the correlated coherence, we find that the local coherence is more robust against thermal noise than the correlated coherence. We have also investigated the effect of imperfect factors on the performance of the ACNC, such as the photon absorption occurring in the FWM processes and unavoidable losses in the light path.

The ACNC has some advantages for recovering quantum coherence. First, its capability for coherence recovery is universal for any input quantum state. This is because the recovery capability is based on the operator level in the Heisenberg picture so the mechanism of recovering coherence is irrelevant to the input states. Second, the ACNC could own larger operational bandwidth, compared with the conventional correlated noisy channels proposed experimentally in Refs. [24–26], which are limited by the electrical bandwidth of the electro-optic modulators used therein. Different from these previous works, the ACNC is all optical so that it avoids the electro-optic conversion. We are hopeful that the ACNC proposed in this paper could be used to study the decoherence effect in quantum optics.

ACKNOWLEDGMENTS

This work is supported by the National Natural Science Foundation of China (Grants No. 12275062, No. 11935012, and No. 61871162), Zhejiang Provincial Natural Science Foundation of China (Grant No. LY24A050004).

-
- [1] T. Baumgratz, M. Cramer, and M. B. Plenio, Quantifying coherence, *Phys. Rev. Lett.* **113**, 140401 (2014).
- [2] A. Streltsov, G. Adesso, and M. B. Plenio, Colloquium: Quantum coherence as a resource, *Rev. Mod. Phys.* **89**, 041003 (2017).
- [3] M.-L. Hu, X. Hu, J. Wang, Y. Peng, Y.-R. Zhang, and H. Fan, Quantum coherence and geometric quantum discord, *Phys. Rep.* **762-764**, 1 (2018).
- [4] A. Streltsov, U. Singh, H. S. Dhar, M. N. Bera, and G. Adesso, Measuring quantum coherence with entanglement, *Phys. Rev. Lett.* **115**, 020403 (2015).
- [5] A. Streltsov, E. Chitambar, S. Rana, M. N. Bera, A. Winter, and M. Lewenstein, Entanglement and coherence in quantum state merging, *Phys. Rev. Lett.* **116**, 240405 (2016).
- [6] E. Chitambar and M.-H. Hsieh, Relating the resource theories of entanglement and quantum coherence, *Phys. Rev. Lett.* **117**, 020402 (2016).

- [7] D. Mondal, T. Pramanik, and A. K. Pati, Nonlocal advantage of quantum coherence, *Phys. Rev. A* **95**, 010301(R) (2017).
- [8] L. Viola, E. Knill, and S. Lloyd, Dynamical decoupling of open quantum systems, *Phys. Rev. Lett.* **82**, 2417 (1999).
- [9] J. Du, X. Rong, N. Zhao, Y. Wang, J. Yang, and R. B. Liu, Preserving electron spin coherence in solids by optimal dynamical decoupling, *Nature (London)* **461**, 1265 (2009).
- [10] G. d. Lange, Z. H. Wang, D. Risté, V. V. Dobrovitski, and R. Hanson, Universal dynamical decoupling of a single solid-state spin from a spin bath, *Science* **330**, 60 (2010).
- [11] P. W. Shor, Scheme for reducing decoherence in quantum computer memory, *Phys. Rev. A* **52**, R2493(R) (1995).
- [12] A. Ekert and C. Macchiavello, Quantum error correction for communication, *Phys. Rev. Lett.* **77**, 2585 (1996).
- [13] C. H. Bennett, D. P. DiVincenzo, J. A. Smolin, and W. K. Wootters, Mixed-state entanglement and quantum error correction, *Phys. Rev. A* **54**, 3824 (1996).
- [14] A. M. Steane, Error correcting codes in quantum theory, *Phys. Rev. Lett.* **77**, 793 (1996).
- [15] D. Gottesman, Class of quantum error-correcting codes saturating the quantum Hamming bound, *Phys. Rev. A* **54**, 1862 (1996).
- [16] E. Knill and R. Laflamme, Theory of quantum error-correcting codes, *Phys. Rev. A* **55**, 900 (1997).
- [17] A. R. R. Carvalho, P. Milman, R. L. de Matos Filho, and L. Davidovich, Decoherence, pointer engineering, and quantum state protection, *Phys. Rev. Lett.* **86**, 4988 (2001).
- [18] H. Mabuchi and P. Zoller, Inversion of quantum jumps in quantum optical systems under continuous observation, *Phys. Rev. Lett.* **76**, 3108 (1996).
- [19] N. Ganesan and T.-J. Tarn, Decoherence control in open quantum systems via classical feedback, *Phys. Rev. A* **75**, 032323 (2007).
- [20] S. S. Sziget, A. R. R. Carvalho, J. G. Morley, and M. R. Hush, Ignorance is bliss: General and robust cancellation of decoherence via no-knowledge quantum feedback, *Phys. Rev. Lett.* **113**, 020407 (2014).
- [21] S. L. Braunstein and P. van Loock, Quantum information with continuous variables, *Rev. Mod. Phys.* **77**, 513 (2005).
- [22] C. Lupo, V. Giovannetti, and S. Mancini, Memory effects in attenuation and amplification quantum processes, *Phys. Rev. A* **82**, 032312 (2010).
- [23] F. Caruso, V. Giovannetti, C. Lupo, and S. Mancini, Quantum channels and memory effects, *Rev. Mod. Phys.* **86**, 1203 (2014).
- [24] X. Deng, S. Hao, C. Tian, X. Su, C. Xie, and K. Peng, Disappearance and revival of squeezing in quantum communication with squeezed state over a noisy channel, *Appl. Phys. Lett.* **108**, 081105 (2016).
- [25] X. Deng, Y. Liu, M. Wang, X. Su, and K. Peng, Sudden death and revival of gaussian Einstein-Podolsky-Rosen steering in noisy channels, *npj Quantum Inf.* **7**, 65 (2021).
- [26] M. Lassen, A. Berni, L. S. Madsen, R. Filip, and U. L. Andersen, Gaussian error correction of quantum states in a correlated noisy channel, *Phys. Rev. Lett.* **111**, 180502 (2013).
- [27] D. Hillerkuss, R. Schmogrow, T. Schellinger, M. Jordan, M. Winter, G. Huber, T. Vallaitis, R. Bonk, P. Kleinow, F. Frey *et al.*, 26 tbit s⁻¹ line-rate super-channel transmission utilizing all-optical fast Fourier transform processing, *Nat. Photon.* **5**, 364 (2011).
- [28] S. Takeda and A. Furusawa, Toward large-scale fault-tolerant universal photonic quantum computing, *APL Photon.* **4**, 060902 (2019).
- [29] H. A. Haus and J. A. Mullen, Quantum noise in linear amplifiers, *Phys. Rev.* **128**, 2407 (1962).
- [30] C. M. Caves, Quantum limits on noise in linear amplifiers, *Phys. Rev. D* **26**, 1817 (1982).
- [31] Y. Yamamoto and H. A. Haus, Preparation, measurement and information capacity of optical quantum states, *Rev. Mod. Phys.* **58**, 1001 (1986).
- [32] A. A. Clerk, M. H. Devoret, S. M. Girvin, F. Marquardt, and R. J. Schoelkopf, Introduction to quantum noise, measurement, and amplification, *Rev. Mod. Phys.* **82**, 1155 (2010).
- [33] J. Xu, Quantifying coherence of Gaussian states, *Phys. Rev. A* **93**, 032111 (2016).
- [34] M. Jasperse, L. D. Turner, and R. E. Scholten, Relative intensity squeezing by four-wave mixing with loss: An analytic model and experimental diagnostic, *Opt. Express* **19**, 3765 (2011).
- [35] V. Boyer, A. M. Marino, R. C. Pooser, and P. D. Lett, Entangled images from four-wave mixing, *Science* **321**, 544 (2008).
- [36] A. M. Marino, R. C. Pooser, V. Boyer, and P. D. Lett, Tunable delay of Einstein-Podolsky-Rosen entanglement, *Nature (London)* **457**, 859 (2009).
- [37] Z. Y. Ou, S. F. Pereira, H. J. Kimble, and K. C. Peng, Realization of the Einstein-Podolsky-Rosen paradox for continuous variables, *Phys. Rev. Lett.* **68**, 3663 (1992).
- [38] J. Kong, F. Hudelist, Z. Y. Ou, and W. Zhang, Cancellation of internal quantum noise of an amplifier by quantum correlation, *Phys. Rev. Lett.* **111**, 033608 (2013).
- [39] C. F. McCormick, V. Boyer, E. Arimondo, and P. D. Lett, Strong relative intensity squeezing by four-wave mixing in rubidium vapor, *Opt. Lett.* **32**, 178 (2007).
- [40] J. Xin, H. Wang, and J. Jing, The effect of losses on the quantum-noise cancellation in the SU(1,1) interferometer, *Appl. Phys. Lett.* **109**, 051107 (2016).
- [41] S. Liu, Y. Lou, J. Xin, and J. Jing, Quantum enhancement of phase sensitivity for the bright-seeded SU(1,1) interferometer with direct intensity detection, *Phys. Rev. Appl.* **10**, 064046 (2018).
- [42] H.-T. Zhou, D.-W. Wang, D. Wang, J.-X. Zhang, and S.-Y. Zhu, Efficient reflection via four-wave mixing in a doppler-free electromagnetically-induced-transparency gas system, *Phys. Rev. A* **84**, 053835 (2011).
- [43] R. Ma, W. Liu, Z. Qin, X. Su, X. Jia, J. Zhang, and J. Gao, Compact sub-kilohertz low-frequency quantum light source based on four-wave mixing in cesium vapor, *Opt. Lett.* **43**, 1243 (2018).
- [44] M. Guo, H. Zhou, D. Wang, J. Gao, J. Zhang, and S. Zhu, Experimental investigation of high-frequency-difference twin beams in hot cesium atoms, *Phys. Rev. A* **89**, 033813 (2014).
- [45] M. T. Turnbull, P. G. Petrov, C. S. Embrey, A. M. Marino, and V. Boyer, Role of the phase-matching condition in nondegenerate four-wave mixing in hot vapors for the generation of squeezed states of light, *Phys. Rev. A* **88**, 033845 (2013).
- [46] H. Y. Ling, Y.-Q. Li, and M. Xiao, Coherent population trapping and electromagnetically induced transparency in multi-Zeeman-sublevel atoms, *Phys. Rev. A* **53**, 1014 (1996).

- [47] J. Choi and D. S. Elliott, Influence of interaction time and population redistribution on the localization of atomic excitation through electromagnetically induced transparency, *Phys. Rev. A* **89**, 013414 (2014).
- [48] Y. Wu, J. Saldana, and Y. Zhu, Large enhancement of four-wave mixing by suppression of photon absorption from electromagnetically induced transparency, *Phys. Rev. A* **67**, 013811 (2003).
- [49] J.-Y. Juo, J.-K. Lin, C.-Y. Cheng, Z.-Y. Liu, I. A. Yu, and Y.-F. Chen, Demonstration of spatial-light-modulation-based four-wave mixing in cold atoms, *Phys. Rev. A* **97**, 053815 (2018).
- [50] B. Do, J. Cha, D. S. Elliot, and S. J. Smith, Degenerate phase-conjugate four-wave mixing in a nearly-doppler-free two-level atomic medium, *Phys. Rev. A* **58**, 3089 (1998).
- [51] R. C. Pooser, A. M. Marino, V. Boyer, K. M. Jones, and P. D. Lett, Quantum correlated light beams from non-degenerate four-wave mixing in an atomic vapor: The D1 and D2 lines of 85Rb and 87Rb, *Opt. Express* **17**, 16722 (2009).
- [52] C. Liu, J. Jing, Z. Zhou, R. C. Pooser, F. Hudelist, L. Zhou, and W. Zhang, Realization of low frequency and controllable bandwidth squeezing based on a four-wave-mixing amplifier in rubidium vapor, *Opt. Lett.* **36**, 2979 (2011).
- [53] Z. Qin, J. Jing, J. Zhou, C. Liu, R. C. Pooser, Z. Zhou, and W. Zhang, Compact diode-laser-pumped quantum light source based on four-wave mixing in hot rubidium vapor, *Opt. Lett.* **37**, 3141 (2012).
- [54] J. Krasinski, D. J. Gauthier, M. S. Malcuit, and R. W. Boyd, Two-photon conical emission, *Opt. Commun.* **54**, 241 (1985).
- [55] A. M. C. Dawes, L. Illing, S. M. Clark, and D. J. Gauthier, All-optical switching in rubidium vapor, *Science* **308**, 672 (2005).
- [56] J. Jing, Z. Zhou, C. Liu, Z. Qin, Y. Fang, J. Zhou, and W. Zhang, Ultralow-light-level all-optical transistor in rubidium vapor, *Appl. Phys. Lett.* **104**, 151103 (2014).
- [57] Y. Lou, S. Liu, and J. Jing, Experimental demonstration of a multifunctional all-optical quantum state transfer machine, *Phys. Rev. Lett.* **126**, 210507 (2021).
- [58] K. McKenzie, E. E. Mikhailov, K. Goda, P. K. Lam, N. Grosse, M. B. Gray, N. Mavalvala, and D. E. McClelland, Quantum noise locking, *J. Opt. B* **7**, S421 (2005).
- [59] Y.-R. Zhang, L.-H. Shao, Y. Li, and H. Fan, Quantifying coherence in infinite-dimensional systems, *Phys. Rev. A* **93**, 012334 (2016).
- [60] A. S. Holevo, M. Sohma, and O. Hirota, Capacity of quantum Gaussian channels, *Phys. Rev. A* **59**, 1820 (1999).
- [61] C. Weedbrook, S. Pirandola, R. García-Patrón, N. J. Cerf, T. C. Ralph, J. H. Shapiro, and S. Lloyd, Gaussian quantum information, *Rev. Mod. Phys.* **84**, 621 (2012).
- [62] C. F. McCormick, A. M. Marino, V. Boyer, and P. D. Lett, Strong low-frequency quantum correlations from a four-wave-mixing amplifier, *Phys. Rev. A* **78**, 043816 (2008).
- [63] J. Xin, J. Qi, and J. Jing, Enhancement of entanglement using cascaded four-wave mixing processes, *Opt. Lett.* **42**, 366 (2017).
- [64] K. C. Tan, H. Kwon, C.-Y. Park, and H. Jeong, Unified view of quantum correlations and quantum coherence, *Phys. Rev. A* **94**, 022329 (2016).
- [65] S. Liu, Y. Lou, and J. Jing, Interference-induced quantum squeezing enhancement in a two-beam phase-sensitive amplifier, *Phys. Rev. Lett.* **123**, 113602 (2019).